

---

# Regularisation Can Mitigate Poisoning Attacks: A Novel Analysis Based on Multiobjective Bilevel Optimisation

---

Javier Carnerero-Cano<sup>1</sup> Luis Muñoz-González<sup>1</sup> Philippa Spencer<sup>2</sup> Emil C. Lupu<sup>1</sup>

## Abstract

Machine Learning (ML) algorithms are vulnerable to poisoning attacks, where a fraction of the training data can be manipulated to deliberately degrade the algorithms performance. Optimal poisoning attacks, which can be formulated as bilevel optimisation problems, help to assess the robustness of learning algorithms in worst-case scenarios. However, current attacks against algorithms with hyperparameters typically assume that these hyperparameters are constant and thus ignore the effect the attack has on them. In this paper, we show that this approach leads to an overly pessimistic view of the robustness of the learning algorithms tested. We propose a novel optimal attack formulation that considers the effect of the attack on the hyperparameters by modelling the attack as a *multiobjective bilevel optimisation problem*. We apply this novel attack formulation to ML classifiers using  $L_2$  regularisation and show that, in contrast to results previously reported in the literature,  $L_2$  regularisation enhances the *stability* of the learning algorithms and helps to partially mitigate poisoning attacks. Our empirical evaluation on different datasets confirms the limitations of previous poisoning attack strategies, evidences the benefits of using  $L_2$  regularisation to dampen the effect of poisoning attacks and shows that the regularisation hyperparameter increases as more malicious data points are injected in the training dataset.

## 1. Introduction

In many applications, Machine Learning (ML) systems rely on data collected from untrusted data sources, such as humans, machines, sensors, or IoT devices that can be compro-

mised and manipulated. Malicious data from these compromised data sources can then be used to poison the learning algorithms. In other applications, the labelling of the training datasets is done manually and *crowdsourcing* techniques are used to aggregate the labelling information from a set of human annotators. In these cases, *crowdturfing* attacks are possible where malicious annotators collude to deceive the crowdsourcing algorithm by manipulating some of the labels of the annotated examples (Yao et al., 2017). All these scenarios expose ML algorithms to poisoning attacks, where adversaries can manipulate a fraction of the training data to subvert the learning process, either to decrease the overall performance or to produce a particular kind of error in the system (Barreno et al., 2010; Huang et al., 2011; Muñoz-González & Lupu, 2019). Poisoning attacks can also facilitate subsequent evasion attacks or produce *backdoor* (or *Trojan*) attacks (Gu et al., 2019; Liu et al., 2017).

Several systematic poisoning attacks have already been proposed to analyse different families of ML algorithms under worst-case scenarios, including Support Vector Machines (SVMs) (Biggio et al., 2012), other linear classifiers (Xiao et al., 2015; Mei & Zhu, 2015; Koh et al., 2018), and neural networks (Koh & Liang, 2017; Muñoz-González et al., 2017). These attack strategies are formulated as a bilevel optimisation problem, i.e. an optimisation problem that *depends* on another optimisation problem. In these cases, the attacker typically aims to maximise some arbitrary malicious objective (e.g. to maximise the error for a set of target data points) by manipulating a fraction of the training data. At the same time, the defender aims to optimise a different objective function to learn the parameters of the model, typically by minimising some loss function evaluated on the poisoned training dataset.

Some of previous attacks target algorithms that have hyperparameters, which are considered as constant regardless of the fraction of poisoning points injected in the training dataset. This can provide a misleading analysis of the robustness of the algorithms against such attacks, as the value of the hyperparameters can change depending on the type and strength of the attack. For example, Xiao et al. (2015) presented a poisoning attack against embedded feature selection methods, including  $L_1$ ,  $L_2$  and *elastic-net*

---

<sup>1</sup>Department of Computing, Imperial College London, London, United Kingdom <sup>2</sup>Defence Science and Technology Laboratory (Dstl), Porton Down, Salisbury, United Kingdom. Correspondence to: Javier Carnerero-Cano <j.cano@imperial.ac.uk>.

regularisation. Their experimental results showed that the attacker can completely control the selection of the features to significantly increase the overall test error of linear classifiers in all cases. However, they assume a constant value for the regularisation hyperparameters regardless of the attack scenario considered in each case. As we show in this paper, this approach can provide overly pessimistic results on the robustness of the learning algorithms to poisoning attacks, as the value of the regularisation hyperparameters significantly changes (if they are optimised) when malicious data points are injected in the training dataset.

In this paper we propose a novel and more general poisoning attack formulation to test worst-case scenarios against ML algorithms that contain hyperparameters. For this, we model the attack as a *multiobjective bilevel optimisation problem*, where the outer objective includes both the learning of the poisoning points and the hyperparameters of the model, whereas the inner problem involves the learning of the model’s parameters. In a worst-case scenario, where the attacker is aware of the dataset used to learn the model’s hyperparameters and aims to maximise the overall error, the outer objective can be modelled as a *minimax* problem.

We applied our proposed attack formulation to test the robustness of ML classifiers that use  $L_2$  regularisation. We used hypergradient descent/ascent to solve the proposed multiobjective bilevel optimisation problem. As the computation of the exact hypergradients can be very expensive, especially for neural networks, we used Reverse-Mode Differentiation (RMD) (Domke, 2012; Maclaurin et al., 2015; Muñoz-González et al., 2017; Franceschi et al., 2018) to approximate the aforementioned hypergradients. Our experimental evaluation shows that, contrary to the results reported by Xiao et al. (2015),  $L_2$  regularisation helps as a mechanism to partially mitigate the effect of poisoning attacks. This is not surprising, as  $L_2$  regularisation is known to increase the stability of the learning algorithm, and thus, can hinder the ability of the attacker to poison the target algorithm. We show that the value of the regularisation hyperparameter increases as the strength of the attack increases. In other words, the algorithm automatically tries to compensate the negative effect of the poisoning points by increasing the strength of the regularisation term. Our proposed attack formulation allows us to appropriately evaluate the robustness of  $L_2$  regularisation in worst-case scenarios.

The rest of the paper is organised as follows: In Sect. 2 we describe the related work. In Sect. 3 we introduce our novel formulation for optimal poisoning attacks against learning algorithms with hyperparameters. In Sect. 4 we discuss how  $L_2$  regularisation can help to mitigate poisoning attacks by enhancing algorithms’ stability. In Sect. 5 we present our experimental evaluation on different datasets. Finally, Sect. 6 concludes the paper.

## 2. Related Work

The first poisoning attacks in the research literature were proposed to target specific applications, such as spam filtering (Nelson et al., 2008; Barreno et al., 2010) or anomaly detection (Barreno et al., 2006; Kloft & Laskov, 2012). A more systematic approach to perform poisoning attacks was introduced by Biggio et al. (2012), introducing an algorithm to poison SVMs modelling the attack as a bilevel optimisation problem. Subsequent works extended this approach to other families of ML algorithms, including linear and other convex classifiers (Mei & Zhu, 2015) or embedded feature selection methods (Xiao et al., 2015). A more general approach was introduced in (Muñoz-González et al., 2017) formulating different optimal attack strategies for targeting multiclass classifiers. The authors also proposed an algorithm to estimate the hypergradients in the corresponding bilevel optimisation problem through RMD, which significantly improves the scalability of optimal attacks, allowing to poison a broader range of learning algorithms, including neural networks. Koh et al. (2018) proposed an algorithm for solving bilevel optimisation problems with detectability constraints, allowing to craft poisoning points that cannot be detected with outlier detectors. However, the algorithm is computationally demanding, which limits its applicability in many practical scenarios.

Other different approaches have also been proposed for crafting poisoning attacks: Koh & Liang (2017) created adversarial training examples by exploiting influence functions. This approach allows to craft successful targeted attacks by injecting small perturbations to genuine data points in the training set. Shafahi et al. (2018) also proposed a targeted poisoning attack for situations where the adversary is not in control of the labels for the poisoning points. Muñoz-González et al. (2019) introduced a generative model to craft poisoning attacks at scale with Generative Adversarial Nets. This approach allows to model naturally detectability constraints for the attacker, enabling attacks with different levels of aggressiveness. This attack is capable of producing indiscriminate and targeted poisoning attacks against different algorithms, including deep networks and bypass different types of existing defences.

On the defender’s side, it is possible to mitigate poisoning attacks by analysing the samples that can have a negative impact on the target algorithms (Nelson et al., 2008). However, this approach can be impractical in many applications, as it offers a poor scalability. Following a similar approach, Koh & Liang (2017) proposed the use of influence function as a mechanism to detect poisoning points. Different outlier detection schemes have been proved to be effective to mitigate poisoning attacks in those cases where the attacker does not model appropriate detectability constraints (Steinhardt et al., 2017; Paudice et al., 2018a). Label sanitisation has

also been proposed as a mechanism to identify and relabel suspicious training data points (Paudice et al., 2018b). However, this strategy fails in attacks where the poisoning points collude, as shown in (Muñoz-González et al., 2019). Finally, Diakonikolas et al. (2019) proposed a meta-algorithm for robust optimisation capable of mitigating some poisoning attacks relying on Singular Vector Decomposition.

### 3. General Optimal Poisoning Attacks

In data poisoning attacks the attacker can tamper with a fraction of the training data points to manipulate the behaviour of the learning algorithm (Barreno et al., 2006; 2010). We assume that the attacker can manipulate all the features and the label of the injected poisoning points, provided that the resulting points are within a feasible domain of valid data points. We also consider white-box attacks with perfect-knowledge, i.e. the attacker knows everything about the target system, including the training data, the feature representation, the loss function, the ML model, and the defence (if applicable) used by the victim. Although unrealistic in most cases, these assumptions for the adversary allow us to analyse the robustness of the ML algorithms in worst-case scenarios for attacks with different strength.

#### 3.1. Problem Formulation

In line with most of the literature in poisoning attacks we consider ML classifiers. Then, in a classification task, given the input space  $\mathcal{X} \in \mathbb{R}^m$  and the label space,  $\mathcal{Y}$ , the learner aims to estimate the mapping  $f : \mathcal{X} \rightarrow \mathcal{Y}$ . Given a training set  $\mathcal{D}_{\text{tr}} = \{(\mathbf{x}_{\text{tr}_i}, y_{\text{tr}_i})\}_{i=1}^{n_{\text{tr}}}$  with  $n_{\text{tr}}$  IID samples drawn from the underlying probability distribution  $p(\mathcal{X}, \mathcal{Y})$ , we can estimate  $f$  with a model  $\mathcal{M}$  trained by minimising an objective function  $\mathcal{L}(\mathcal{D}_{\text{tr}}, \mathbf{w}, \Lambda)$ , w.r.t. its parameters  $\mathbf{w} \in \mathbb{R}^d$ , given a set of hyperparameters  $\Lambda \in \mathbb{R}^c$ .

We also assume that the defender has access to a validation dataset  $\mathcal{D}_{\text{val}} = \{(\mathbf{x}_{\text{val}_j}, y_{\text{val}_j})\}_{j=1}^{n_{\text{val}}}$  with  $n_{\text{val}}$  trusted data points. Then, as proposed by Foo et al. (2008), the model’s hyperparameters can be learned by solving the following bilevel optimisation problem:

$$\begin{aligned} \min_{\Lambda \in \Phi(\Lambda)} \quad & \mathcal{L}(\mathcal{D}_{\text{val}}, \mathbf{w}^*) \\ \text{s.t.} \quad & \mathbf{w}^* \in \arg \min_{\mathbf{w} \in \mathcal{W}} \mathcal{L}(\mathcal{D}_{\text{tr}}, \mathbf{w}, \Lambda), \end{aligned} \quad (1)$$

where  $\Phi(\Lambda)$  represent the feasible domain set for the hyperparameters  $\Lambda$ .

On the other side, in a poisoning attack, the adversary aims to inject a set of  $n_{\text{p}}$  malicious data points,  $\mathcal{D}_{\text{p}} = \{(\mathbf{x}_{\text{p}_k}, y_{\text{p}_k})\}_{k=1}^{n_{\text{p}}}$ , in the training dataset to maximise some arbitrary objective,  $\mathcal{A}$ , evaluated on a set of target data points  $\mathcal{D}_{\text{target}}$ . As described in (Muñoz-González et al., 2017) different attack scenarios can be considered depending on both

the set of target data points and the attacker’s objective, including indiscriminate and targeted attacks. In these settings, we propose to formulate the problem for the attacker as the multiobjective bilevel optimisation problem:

$$\begin{aligned} \min_{\Lambda \in \Phi(\Lambda)} \quad & \mathcal{L}(\mathcal{D}_{\text{val}}, \mathbf{w}^*), \max_{\mathcal{D}_{\text{p}} \in \Phi(\mathcal{D}_{\text{p}})} \mathcal{A}(\mathcal{D}_{\text{target}}, \mathbf{w}^*) \\ \text{s.t.} \quad & \mathbf{w}^* \in \arg \min_{\mathbf{w} \in \mathcal{W}} \mathcal{L}(\mathcal{D}'_{\text{tr}}, \mathbf{w}, \Lambda), \end{aligned} \quad (2)$$

where  $\mathcal{D}'_{\text{tr}} = \mathcal{D}_{\text{tr}} \cup \mathcal{D}_{\text{p}}$  is the poisoned dataset and  $\Phi(\mathcal{D}_{\text{p}})$  is the feasible domain set for the injected poisoning points, i.e. the attacker’s constraints.

Previous work in the research literature have neglected the effect of the hyperparameters in the problem for the attacker, e.g. the regularisation hyperparameter for the cost function for SVMs (Biggio et al., 2012) or for embedded feature selection methods (Xiao et al., 2015). From the general formulation we propose in (2) it is clear that the poisoning points in  $\mathcal{D}'_{\text{tr}}$  have an effect not only on the weights of the classifier, but also on its hyperparameters. Then, testing the robustness of the learning algorithms with attacks that ignore this effect can produce misleading results, as we show, for example, in the synthetic experiment in Fig. 1 for the case of  $L_2$  regularisation. Thus, if we ignore the effect on the hyperparameters, these attacks can overestimate the adversary’s capabilities to influence the learning algorithm.

Our novel attack formulation in (2) allows to model a wide variety of attack scenarios, depending on the attacker’s objective and the combinations between the target, validation and training data points. In the remainder of the paper we will focus on analysing worst-case scenarios for indiscriminate poisoning attacks, i.e. those where the attacker aims to increase the overall classification error in the target system. To achieve such a goal in this case, the attacker would aim to maximise the loss evaluated on the validation dataset, i.e.  $\mathcal{A}(\mathcal{D}_{\text{target}}, \mathbf{w}^*) = \mathcal{L}(\mathcal{D}_{\text{val}}, \mathbf{w}^*)$ . Then, the problem for the attacker can also be formulated as a bilevel optimisation problem where the outer objective is a minimax problem:

$$\begin{aligned} \min_{\Lambda \in \Phi(\Lambda)} \quad & \max_{\mathcal{D}_{\text{p}} \in \Phi(\mathcal{D}_{\text{p}})} \mathcal{L}(\mathcal{D}_{\text{val}}, \mathbf{w}^*) \\ \text{s.t.} \quad & \mathbf{w}^* \in \arg \min_{\mathbf{w} \in \mathcal{W}} \mathcal{L}(\mathcal{D}'_{\text{tr}}, \mathbf{w}, \Lambda). \end{aligned} \quad (3)$$

None of previous approaches described in the research literature have modelled attacks as multiobjective bilevel optimisation problems as in (2) and (3). Beyond the scope of our paper, our approach can also be useful to test the robustness of defensive algorithms to data poisoning in worst-case scenarios when those algorithms contain parameters.

#### 3.2. Solving General Optimal Poisoning Attacks

Solving the multiobjective bilevel optimisation problems in (2) and (3) is strongly NP-Hard (Bard, 2013) and, even

if the inner problem is convex, the outer problem is, in general, non-convex. However, it is possible to use gradient-based approaches to get (possibly) suboptimal solutions, i.e. finding local optima for the problem in (2) and saddle points for the minimax problem in (3). For the sake of clarity, in the remainder we will focus on the solution for the problem (3), as we will use it in our experiments to show the robustness of  $L_2$  regularisation to indiscriminate poisoning attacks. The solution of (2) follows a similar procedure.

In order to compute the hypergradients for the outer objective, we assume that the loss function,  $\mathcal{L}$ , is convex and its first and second derivatives are Lipschitz-continuous functions. Similar to (Biggio et al., 2012; Mei & Zhu, 2015; Xiao et al., 2015; Muñoz-González et al., 2017) we assume that the label of the poisoning points is set a priori, so the attacker just need to learn the features for the poisoning points,  $\mathbf{X}_p$ . For the sake of clarity we will use  $\mathcal{A}$  to denote the loss function evaluated on the validation dataset in the outer objective, i.e.  $\mathcal{L}(\mathcal{D}_{\text{val}}, \mathbf{w})$ , and  $\mathcal{L}$  to refer to the loss function evaluated on the training data in the inner objective, i.e.  $\mathcal{L}(\mathcal{D}'_{\text{tr}}, \mathbf{w})$ . We can compute the hypergradients in the outer optimisation problem by leveraging the conditions for stationarity in the inner problem, i.e.  $\nabla_{\mathbf{w}}\mathcal{L} = \mathbf{0}$ , and applying the implicit function theorem (Mei & Zhu, 2015). Then, the hypergradients can be computed as:

$$\begin{aligned}\nabla_{\mathbf{X}_p}\mathcal{A} &= -(\nabla_{\mathbf{X}_p}\nabla_{\mathbf{w}}\mathcal{L})^\top (\nabla_{\mathbf{w}}^2\mathcal{L})^{-1} \nabla_{\mathbf{w}}\mathcal{A}, \\ \nabla_{\Lambda}\mathcal{A} &= -(\nabla_{\Lambda}\nabla_{\mathbf{w}}\mathcal{L})^\top (\nabla_{\mathbf{w}}^2\mathcal{L})^{-1} \nabla_{\mathbf{w}}\mathcal{A},\end{aligned}\quad (4)$$

where we assume that the Hessian  $\nabla_{\mathbf{w}}^2\mathcal{L}$  is not singular. Brute-force computation of (4) requires inverting the Hessian, which scales in time as  $\mathcal{O}(d^3)$  and in memory as  $\mathcal{O}(d^2)$ —where  $d$  is the dimensionality of the weights. However, as proposed by Foo et al. (2008), we can rearrange the terms in the second part of (4) and solve first the linear system:  $(\nabla_{\mathbf{w}}^2\mathcal{L})\mathbf{v} = \nabla_{\mathbf{w}}\mathcal{A}$ , and then, compute  $\nabla_{\mathbf{X}_p}\mathcal{A} = -(\nabla_{\mathbf{X}_p}\nabla_{\mathbf{w}}\mathcal{L})^\top \mathbf{v}$ .<sup>1</sup> The linear system can be efficiently solved by using conjugate gradient descent, reducing the complexity to compute the hypergradients. Matrix vector products can also be efficiently computed with the approximations proposed by Pearlmutter (1995), avoiding the computation of the Hessian.

However, the previous approach requires to solve the inner optimisation problem, i.e. training the whole learning algorithm, to compute the hypergradient in the outer problem. This can be computationally prohibitive in the case of some learning algorithms such as deep networks, where the number of parameters is huge. To sidestep this problem, different techniques have been proposed to estimate the value of the hypergradients in bilevel optimisation problems (Domke,

2012; Maclaurin et al., 2015; Pedregosa, 2016; Franceschi et al., 2017; Muñoz-González et al., 2017; Franceschi et al., 2018). These techniques do not require to re-train the learning algorithm every time the hypergradient is computed in the outer problem. Instead, they provide an estimate of the hypergradient by truncating the learning in the inner problem to a reduced number of epochs.

As described by Franceschi et al. (2017), we can think of the training algorithm as a discrete-time dynamical system, described by a set of states  $\mathbf{s}^{(t)} \in \mathbb{R}^{d_s}$ , with  $t = 0, \dots, T$ , where each state depends on  $\mathbf{w}$ , the accumulated gradients and/or the velocities. Then, from a reduced number of training iterations,  $T$ , we can estimate the hypergradients from the values of the parameters collected in the set of states. Depending on the order to compute the operations we can differentiate two approaches to estimate the hypergradients: Reverse-Mode (RMD) and Forward-Mode Differentiation (FMD) (Griewank & Walther, 2008; Franceschi et al., 2017). In the first case, RMD requires first to train the learning algorithm for  $T$  epochs, and then, to compute  $\mathbf{s}^{(0)}$  to  $\mathbf{s}^{(T)}$ . Then, the hypergradients estimate is computed by reversing the steps followed by the learning algorithm from  $\mathbf{s}^{(T)}$  down to  $\mathbf{s}^{(0)}$ . On the other hand, FMD computes the estimate of the hypergradients as the algorithm is trained, i.e. from  $\mathbf{s}^{(0)}$  to  $\mathbf{s}^{(T)}$  (i.e. the estimates can be computed in parallel with the training procedure).

In some cases, as in (Domke, 2012), RMD requires to store all the information collected in the states in the forward pass. This can be prohibitive in some cases as, for example, for deep networks where the number of parameters is huge. However, other RMD methods proposed in the literature do not require to store this information (Maclaurin et al., 2015; Muñoz-González et al., 2017). To estimate the hypergradients RMD requires to compute a forward and a backward pass through the set of states. In contrast, FMD just needs to do the forward computation. However, the scalability of FMD depends heavily on the number of hyperparameters compared to RMD. Then, for problems where the number of hyperparameters is large, as it is the case for the poisoning attacks we introduced in (2) and (3), RMD is computationally more efficient to estimate the hypergradients. For this reason, we used RMD in our experiments.

Finally, once we have computed the exact or the approximate hypergradients, at each hyperiteration we can use projected hypergradient descent/ascent to update the value of the poisoning points and the model's hyperparameters:

$$\begin{aligned}\mathbf{X}_p &\leftarrow \Pi_{\Phi(\mathbf{X}_p)}(\mathbf{X}_p + \alpha \nabla_{\mathbf{X}_p}\mathcal{A}), \\ \Lambda &\leftarrow \Pi_{\Phi(\Lambda)}(\Lambda - \beta \nabla_{\Lambda}\mathcal{A}),\end{aligned}\quad (5)$$

where  $\alpha$  and  $\beta$  are respectively the learning rates and  $\Pi_{\Phi(\mathbf{X}_p)}$  and  $\Pi_{\Phi(\Lambda)}$  are the projection operators for the poisoning points,  $\mathbf{X}_p$ , and the hyperparameters,  $\Lambda$ , so that their up-

<sup>1</sup> The resulting expression for the case of  $\Lambda$  is analogous.

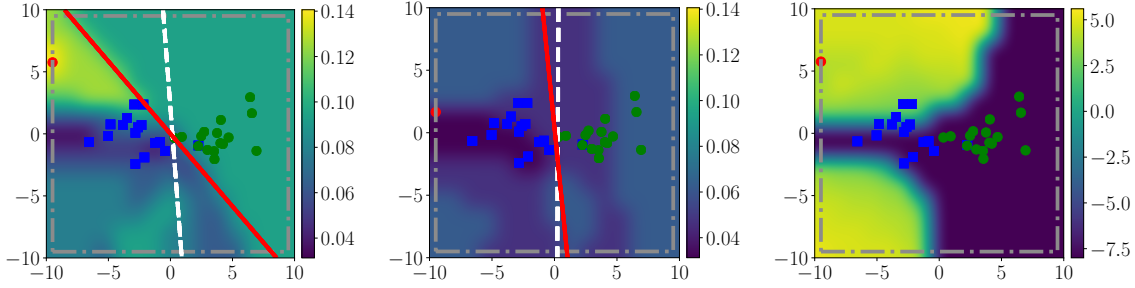


Figure 1. Effect of regularisation on a synthetic example. The blue and green points represent the training data points for each class, and the red point is the poisoning point (labelled as green). The dashed-dotted grey box represent the attacker’s constraints. Dashed-white lines and solid-red lines depict the decision boundaries for LR classifiers trained on clean and tainted datasets respectively. (Left) Standard LR with no regularisation. (Centre) LR with  $L_2$  regularisation. The colour-maps in the two plots represent the validation error as a function of the poisoning point. (Right) Value of  $\lambda$  learned by solving (1) as a function of the injected poisoning point.

dated values are within the corresponding feasible domains,  $\Phi(\mathbf{X}_p)$  and  $\Phi(\Lambda)$ . In our case we used standard gradient ascent/descent to solve (3). The analysis of other alternatives to solve minimax games, such as *optimistic gradient descent/ascent* (Daskalakis & Panageas, 2018) is left for future work.

#### 4. $L_2$ Regularisation to Mitigate Poisoning Attacks

Poisoning attacks are intrinsically related to the stability of the learning algorithms. Attackers aim to manipulate the model by compromising a small fraction of the training data. In other words, they aim to produce large changes in the target algorithm by influencing a reduced set of training points. Xu et al. (2011) introduced the following definition of stability: “an ML algorithm is stable if its output is nearly identical on two datasets, differing on only one sample.” This concept of stability has also been studied in the field of robust statistics, in which robustness formally denotes this notion of stability (Rubinstein et al., 2009). It is not our intention here to provide a formal analysis on the stability of the learning algorithms, but to show that stability is an important property for the design of learning algorithms robust to data poisoning. For instance, Muñoz-González et al. (2019) showed empirically that for the same fraction of malicious points in the training set, the effect of a poisoning attack reduces when we increase the number of training points, as the stability of the algorithm increases. Therefore, data augmentation can be helpful to limit the ability of the attacker to degrade overall system’s performance, leading to significant improvements in generalisation (Simard et al., 2003). However data augmentation may not be as effective to defend against more targeted attacks or backdoors.

$L_2$  (or Tikhonov) regularisation is a well-known mechanism to increase the stability of ML algorithms (Xu et al., 2011). In  $L_2$  regularisation we add a penalty term to the

original loss function which shrinks the norm of the model’s parameters, so that:

$$\mathcal{L}'(\mathcal{D}_{tr}, \mathbf{w}, \lambda) = \mathcal{L}(\mathcal{D}_{tr}, \mathbf{w}) + \frac{e^\lambda}{2} \|\mathbf{w}\|_2^2, \quad (6)$$

where  $\lambda$  is the hyperparameter that controls the strength of the regularisation term. The exponential form is used to ensure a positive contribution of the regularisation term for  $\mathcal{L}'$  and to help learning  $\lambda$ , for example by using (1), as this hyperparameter is usually searched over a log-spaced grid (Pedregosa, 2016). Different  $L_2$  regularisation schemes can be considered. For example, in neural networks, we can have one penalty term for the parameters at each layer or, more generally, we can have a different regularisation term for each parameter in the model (Foo et al., 2008).

Xiao et al. (2015) analysed the robustness of embedded feature selection, including  $L_2$  regularisation, for linear classifiers against optimal poisoning attacks. Although the reported experimental results showed that  $L_2$  regularisation was slightly more robust compared to  $L_1$  regularisation and *elastic-net*, all the tested classifiers were significantly vulnerable to indiscriminate optimal poisoning attacks. However, these results relied on the assumption that the regularisation hyperparameter was constant regardless of the fraction of training data points. This approach can produce misleading results, as the poisoning points can have a significant effect on the value of the hyperparameter learned, for example by using (1).

In Fig. 1 we show a synthetic example with a binary classification problem to illustrate the limitations of the approach considered by Xiao et al. (2015). In the example, the data points for the two classes were drawn from two different bivariate Gaussian distributions and we trained a Logistic Regression (LR) classifier. In Fig. 1(left) we show the effect of a poisoning attack against an LR classifier with no regularisation, trained with 32 data points (16 per class), injecting a single poisoning point (labelled as red) that aims

to maximise the error measured on a separate validation set with 64 data points.<sup>2</sup> The dashed-dotted grey box depicts the constraints imposed for the attacker to craft the poisoning point. The dashed-white line represents the decision boundary learned when training on the clean dataset, whereas the red line depicts the decision boundary of the LR trained on the poisoned dataset. We can observe that, in this case, one single poisoning point can significantly alter the decision boundary. In Fig. 1(centre), we show a similar scenario, but training an LR classifier with  $L_2$  regularisation, setting  $\lambda = \log(20) \approx 3$ . In this case, we can observe that the effect of the poisoning point on the classifier trained on the poisoned dataset is very reduced and its decision boundary shifts just slightly. In the background of these two figures we represent the error evaluated on the validation set for the LR trained on a poisoned dataset as a function of the location of the poisoning point. We can observe that, when there is no regularisation (left) the error can significantly increase when we inject the poisoning point in certain regions. On the contrary, when regularisation is applied (centre), the colour-map is more uniform, i.e. the algorithm is quite stable regardless of the position of the poisoning point and the increase in the validation error after the attack is very small.

In Fig. 1(right) we show how the value of the regularisation hyperparameter,  $\lambda$ , changes as a function of the poisoning point. The colour-map in the background represents the value of  $\lambda$  learned by solving (1), i.e. the  $\lambda$  that minimises the error on the validation set. We can observe that the value for  $\lambda$  can change significantly depending on the position of the poisoning point. Thus, the value of  $\lambda$  is much bigger for the regions where the poisoning point can influence more the classifier (see Fig. 1(left)). In other words, when the poisoning attack can have a very negative impact on the classifier’s performance, the importance of the regularisation term, controlled by  $\lambda$ , increases. It is clear that selecting appropriately the value of  $\lambda$  can have a significant impact on the robustness of the classifier. Then, when testing the robustness of  $L_2$  regularised classifiers we must consider the interplay between the strength of the poisoning attack and the value of the regularisation hyperparameter.

## 5. Experiments

In this section, we evaluate the effectiveness of the attack strategy in (3) against LR and feed-forward Deep Neural Networks (DNNs).<sup>3</sup> For LR, we use three different binary classification problems: MNIST (‘0’ vs ‘8’) (Le-Cun et al., 1998), Fashion-MNIST (FMNIST) (*T-shirt vs pullover*) (Xiao et al., 2017), and ImageNet (*dog vs fish*)

<sup>2</sup> The complete details of the experiment can be found in Appendix D.

<sup>3</sup> All the experiments were run on  $2 \times 11$ GB NVIDIA GeForce® GTX 1080 Ti GPUs.

(Russakovsky et al., 2015) preprocessed as in (Koh & Liang, 2017), where the first two datasets have 784 features, and the latter one has 2,048 features. For the DNN, we focus on ImageNet. For all datasets, we use 512 training and validation points respectively, drawn at random from the original pool of training points for these datasets. For testing, we use 1,954 points for MNIST, 2,000 for FMNIST, and 600 for ImageNet. All the results in our experiments are the average of 10 repetitions with different random data splits for the training and validation sets. The rest of the details about the experimental setup are described in Appendix D. We choose RMD as the number of hyperparameters to be learned is big, which makes RMD a more efficient approach to compute the hypergradients compared to FMD.

### 5.1. Logistic Regression

For LR we test the general poisoning attack strategy in (3) using the following settings for the computation of the hypergradients with RMD: For MNIST we set  $T$ , the number of iterations for the inner optimisation problem, to 150. For FMNIST and ImageNet we use  $T = 180$  and  $T = 200$  respectively. For comparison purposes, we crafted optimal poisoning attacks, setting the value of the regularisation parameter to different constant values: A very small regularisation term  $\lambda = -8$ , a very large regularisation term ( $\lambda = \log(200)$  for MNIST,  $\lambda = \log(500)$  for FMNIST, and  $\lambda = \log(3,000)$  for ImageNet), and the value of  $\lambda$  learned with 5-fold cross-validation, training the algorithm on the clean dataset ( $\lambda_{\text{CLEAN}}$ ). The last case is similar to the experimental settings used by (Xiao et al., 2015). For all the attacks we measure the average test error over 10 independent splits for different attack strength, varying the number of poisoning points from 0 to 85. The results are shown in Fig. 2(a)-(c). We can observe that for the small  $\lambda$  and  $\lambda_{\text{CLEAN}}$  the attacks are very effective and the test error significantly increases when compared to the algorithm’s performance on the clean dataset. In contrast, for the biggest  $\lambda$  the test error slightly increases with the increasing fraction of poisoning points, showing a very stable performance regardless of the attack strength. However, in the absence of an attack, the algorithm clearly *underfits* and the error is significantly higher compared to the other models. When we adapt the value of  $\lambda$  as a function of the attack strength ( $\lambda_{\text{RMD}}$ ), i.e. solving the problem in (3), we can see that the increase on the test error is quite moderate and stabilises at some point. In other words, the error does not increase further by injecting more poisoning points. In the absence of attack, we can observe that the performance for  $\lambda_{\text{RMD}}$  is as good as in the case of  $\lambda_{\text{CLEAN}}$ .

The results in Fig. 2(a)-(c) show that the attack and the methodology presented in (Xiao et al., 2015) provide an overly pessimistic view on the robustness of  $L_2$  regularisation to data poisoning attacks and that, by appropriately

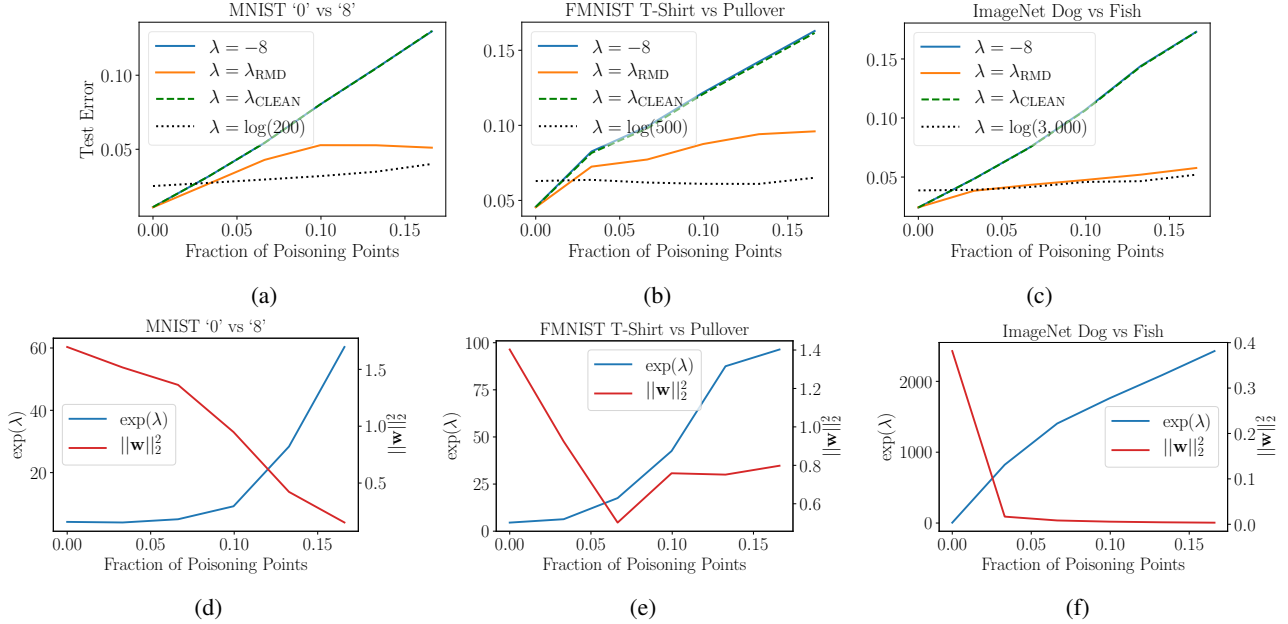


Figure 2. Results for the optimal attack against LR: The first row represents the average test error on (a) MNIST, (b) FMNIST, and (c) ImageNet. The second row contains the plots for  $\lambda$  and  $\|\mathbf{w}\|_2^2$  for (d) MNIST, (e) FMNIST, and (f) ImageNet.

selecting the value of  $\lambda$ , we can effectively reduce the impact of such attacks. Second, we can also observe that there exists a trade-off between accuracy and robustness: Thus, over-regularising (i.e. setting a very large value for  $\lambda$ ) makes the algorithm more robust to the attack, but the performance is degraded when there is no attack.

In Fig. 2(d)-(f) we show the value of  $\lambda$  learned and the norm of the model’s weights,  $\|\mathbf{w}\|_2^2$ , as a function of the fraction of poisoning points injected for the solution of problem (3) with RMD. We can observe that in all cases, the regularisation parameter increases as we increase the fraction of poisoning points, which means that the regulariser tries to compensate the effect of the malicious samples on the model’s weights. Thus, as expected,  $L_2$  provides a natural mechanism to stabilise the model in the presence of attacks. In the case of ImageNet, the order of magnitude of  $\lambda$  is higher as there are more features in the model. On the other side, in Fig. 2(d)-(f) we can also observe that, as expected from (6), when  $\lambda$  increases, the norm of the weights decreases.

## 5.2. Deep Neural Networks

For DNNs, we consider a vector of regularisation hyperparameters  $\lambda$ , with one hyperparameter for each layer. In the case of DNNs, one of the limitations of having a single regularisation hyperparameter is its inconsistency with certain scaling properties across the layer mappings. Intuitively, the amount of scaling needed by each layer’s weights to compensate for a change in the output is not the same, given the

nonlinear activation functions. Therefore, we use a different regularisation penalty term at each layer. This can also give us an intuition about which layer is more vulnerable to the poisoning attack. For the DNNs we also propose an additional modification for the RMD algorithm: We apply different initial random states  $\mathbf{w}^{(0)}$  for every update of the poisoning points. This can be interpreted as assembling different randomly initialised DNNs to improve the generalisation of the poisoning points across different parameter initialisations. In this case we set  $T = 600$ . This scenario is much more challenging for the multiobjective bilevel problem we aim to solve, as the model has two hidden layers ( $2, 048 \times 128 \times 32 \times 1$ ) with Leaky ReLU activation functions, which sums up to a total of 266, 433 parameters (including the bias terms).

As in the previous experiment, we performed attacks with different strengths for the DNN trained with small ( $\lambda = -8$ ) and large ( $\lambda = \log(40)$ ) values for the regularisation hyperparameter, constant for all the layers. In this case, we omitted the case where  $\lambda$  is set by 5-fold cross-validation on the clean dataset as the search space is large, which makes it computationally very expensive. As before, we denote with  $\lambda_{\text{RMD}}$  the case where the regularisation hyperparameter is learned as a function of the poisoning points by solving (3). The results in Fig. 3(a) are consistent with those obtained for the case of LR: For  $\lambda = -8$  the algorithm is very vulnerable to the poisoning attack and its test error significantly increases up to 15% when the training dataset is poisoned with 16.6% malicious points. On the contrary, for  $\lambda = \log(40)$  the algorithm’s performance remains quite

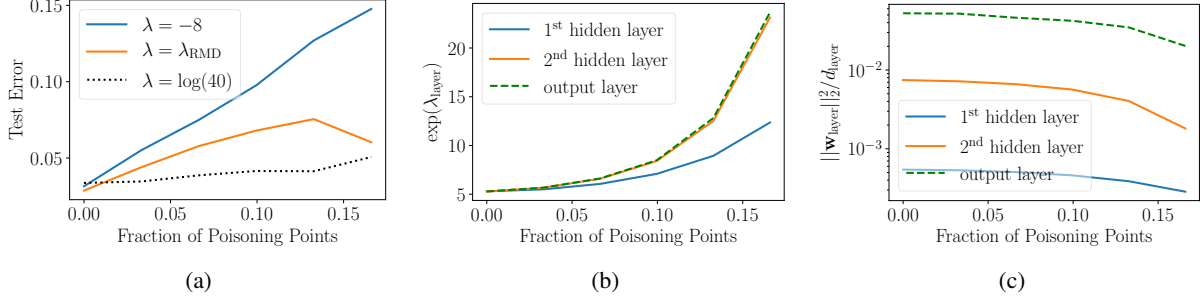


Figure 3. Results for the optimal attack against the DNN on ImageNet. (a) Test error.  $\lambda_{\text{RMD}}$  represents the one computed with RMD. (b)  $\lambda$  computed with RMD. (c)  $\|\mathbf{w}_{\text{layer}}\|_2^2/d_{\text{layer}}$ , where  $d_{\text{layer}}$  represents the number of parameters of the corresponding layer. This normalisation allows comparing  $\|\mathbf{w}_{\text{layer}}\|_2^2$  for each layer regardless of the number of the parameters.

stable for increasing fractions of poisoning points. For  $\lambda_{\text{RMD}}$  the test error increases moderately and reaches a maximum when the fraction of poisoning points is 13%. After that, the error slightly decreases when the fraction of poisoning points increases. This interesting behaviour can be explained from the results in Fig. 3(b) where we show the values of  $\lambda$  learned for each layer as a function of the attack strength. We can observe that there is a significant increase of the regularisation parameter learned for the second and the output layers when the fraction of poisoning points is larger than 13%. This significant increase on the regularisation terms can imply an important change in the decision boundary of the DNN, which, in this particular case, makes it more robust to the poisoning attack despite the fraction of poisoning points is larger. Finally, from Fig. 3(a) we can see that when there is no attack, the test error for  $\lambda_{\text{RMD}}$  is smaller than the other two cases. As discussed before, although over-regularising may be appealing to make the algorithm more robust to poisoning attacks, the performance in the absence of attack may be significantly worse.

In Fig. 3(b) we can observe that the  $\lambda$  learned for the second and output layers increase faster than the one for the first layer. This result suggests that the latter layers are more vulnerable to the poisoning attack. In other words, the poisoning attack tries to produce more changes in the parameters of the network in those layers and, at the same time, the network tries to resist to those changes by increasing the value of the corresponding regularisation parameters. Finally, in Fig. 3(c) we show the  $L_2$  norm of the weights for each layer divided by the number of parameters in each case. The results are consistent with those in Fig. 3(b): The norm of the weights in the last two layers significantly decrease when we increase the fraction of poisoning points. On the other side, regardless of the attack strength, the norm of the weights is significantly bigger for the output layer.

## 6. Conclusions

In this paper we introduce a novel poisoning attack strategy for evaluating the robustness of ML classifiers that contain hyperparameters in worst-case scenarios. The attack can be formulated as a multiobjective bilevel optimisation problem that can be solved with gradient-based approaches by computing the exact hypergradients (making use of the implicit function theorem) or by estimating these hypergradients efficiently with RMD or FMD methods. We show the limitations of previous approaches, such as those described by Biggio et al. (2012); Xiao et al. (2015), where the model’s hyperparameters are considered to be constant regardless of the type and strength of the attack. As we show in our experiments with synthetic and real data, this approach can provide a misleading (and often pessimistic) view of the robustness of the algorithms. Our experiments show that these poisoning attacks can have a strong influence on the value learned for the hyperparameters, and thus, their influence must be considered when assessing the robustness of the algorithms to worst-case attacks.

We also show that, contrary to the results reported by Xiao et al. (2015),  $L_2$  regularisation can help to mitigate the effect of poisoning attacks, increasing the stability of the learning algorithms. Then, when the attacker increases the strength of the attack the regularisation hyperparameter also increases to compensate the instability that the attacker tries to produce in the algorithm. Our experimental evaluation shows the benefits of using  $L_2$  regularisation as a good practice to reduce the impact of poisoning attacks. We also illustrate the trade-off between robustness and accuracy as a function of the regularisation hyperparameter. Our results highlight the importance of stability as a desired property for the design of more robust algorithms to data poisoning. Further research work will include the analysis of other forms of regularisation, such as  $L_1$  and elastic-net, and the analysis of the robustness to data poisoning for other learning algorithms that contains hyperparameters, including the SVM.



## References

- Bard, J. F. *Practical Bilevel Optimization: Algorithms and Applications*, volume 30. Springer Science & Business Media, 2013.
- Barreno, M., Nelson, B., Sears, R., Joseph, A. D., and Tygar, J. D. Can Machine Learning Be Secure? In *Proceedings of the 2006 ACM Symposium on Information, Computer and Communications Security*, pp. 16–25. ACM, 2006.
- Barreno, M., Nelson, B., Joseph, A. D., and Tygar, J. D. The security of machine learning. *Machine Learning*, 81(2):121–148, 2010.
- Biggio, B., Nelson, B., and Laskov, P. Poisoning Attacks against Support Vector Machines. In *International Conference on Machine Learning*, pp. 1807–1814, 2012.
- Daskalakis, C. and Panageas, I. The Limit Points of (Optimistic) Gradient Descent in Min-Max Optimization. In *Advances in Neural Information Processing Systems*, pp. 9236–9246, 2018.
- Diakonikolas, I., Kamath, G., Kane, D., Li, J., Steinhardt, J., and Stewart, A. Sever: A Robust Meta-Algorithm for Stochastic Optimization. In *International Conference on Machine Learning*, pp. 1596–1606, 2019.
- Domke, J. Generic Methods for Optimization-Based Modeling. In *Artificial Intelligence and Statistics*, pp. 318–326, 2012.
- Foo, C.-S., Do, C. B., and Ng, A. Y. Efficient multiple hyperparameter learning for log-linear models. In *Advances in Neural Information Processing Systems*, pp. 377–384, 2008.
- Franceschi, L., Donini, M., Frasconi, P., and Pontil, M. Forward and Reverse Gradient-Based Hyperparameter Optimization. In *International Conference on Machine Learning*, pp. 1165–1173, 2017.
- Franceschi, L., Frasconi, P., Salzo, S., Grazzi, R., and Pontil, M. Bilevel Programming for Hyperparameter Optimization and Meta-Learning. In *International Conference on Machine Learning*, pp. 1568–1577, 2018.
- Griewank, A. and Walther, A. *Evaluating Derivatives: Principles and Techniques of Algorithmic Differentiation*, volume 105. SIAM, 2008.
- Gu, T., Liu, K., Dolan-Gavitt, B., and Garg, S. BadNets: Evaluating Backdooring Attacks on Deep Neural Networks. *IEEE Access*, 7:47230–47244, 2019.
- Huang, L., Joseph, A. D., Nelson, B., Rubinstein, B. I., and Tygar, J. Adversarial Machine Learning. In *Proceedings of the 4th ACM Workshop on Security and Artificial Intelligence*, pp. 43–58. ACM, 2011.
- Kloft, M. and Laskov, P. Security Analysis of Online Centroid Anomaly Detection. *Journal of Machine Learning Research*, 13(Dec):3681–3724, 2012.
- Koh, P. W. and Liang, P. Understanding Black-box Predictions via Influence Functions. In *International Conference on Machine Learning*, pp. 1885–1894, 2017.
- Koh, P. W., Steinhardt, J., and Liang, P. Stronger Data Poisoning Attacks Break Data Sanitization Defenses. *arXiv preprint arXiv:1811.00741*, 2018.
- LeCun, Y., Bottou, L., Bengio, Y., Haffner, P., et al. Gradient-Based Learning Applied to Document Recognition. *Proceedings of the IEEE*, 86(11):2278–2324, 1998.
- Liu, Y., Ma, S., Aafer, Y., Lee, W.-C., Zhai, J., Wang, W., and Zhang, X. Trojaning Attack on Neural Networks. In *Department of Computer Science Technical Reports, Purdue University*, 2017.
- Maclaurin, D., Duvenaud, D., and Adams, R. Gradient-based Hyperparameter Optimization through Reversible Learning. In *International Conference on Machine Learning*, pp. 2113–2122, 2015.
- Mei, S. and Zhu, X. Using Machine Teaching to Identify Optimal Training-Set Attacks on Machine Learners. In *Proceedings of the Twenty-Ninth AAAI Conference on Artificial Intelligence*, pp. 2871–2877, 2015.
- Muñoz-González, L. and Lupu, E. C. The Security of Machine Learning Systems. In *AI in Cybersecurity*, pp. 47–79. Springer, 2019.
- Muñoz-González, L., Biggio, B., Demontis, A., Paudice, A., Wongrassamee, V., Lupu, E. C., and Roli, F. Towards Poisoning of Deep Learning Algorithms with Back-gradient Optimization. In *Proceedings of the 10th ACM Workshop on Artificial Intelligence and Security*, pp. 27–38. ACM, 2017.
- Muñoz-González, L., Pfützner, B., Russo, M., Carnerero-Cano, J., and Lupu, E. C. Poisoning Attacks with Generative Adversarial Nets. *arXiv preprint arXiv:1906.07773*, 2019.
- Nelson, B., Barreno, M., Chi, F. J., Joseph, A. D., Rubinstein, B. I., Saini, U., Sutton, C. A., Tygar, J. D., and Xia, K. Exploiting Machine Learning to Subvert Your Spam Filter. *LEET*, 8:1–9, 2008.
- Paudice, A., Muñoz-González, L., György, A., and Lupu, E. C. Detection of Adversarial Training Examples in Poisoning Attacks through Anomaly Detection. *arXiv preprint arXiv:1802.03041*, 2018a.

- Paudice, A., Muñoz-González, L., and Lupu, E. C. Label Sanitization Against Label Flipping Poisoning Attacks. In *Joint European Conference on Machine Learning and Knowledge Discovery in Databases*, pp. 5–15. Springer, 2018b.
- Pearlmutter, B. A. Fast Exact Multiplication by the Hessian. *Neural Computation*, 6(1):147–160, 1994.
- Pearlmutter, B. A. Gradient Calculations for Dynamic Recurrent Neural Networks: A Survey. *IEEE Transactions on Neural Networks*, 6(5):1212–1228, 1995.
- Pedregosa, F. Hyperparameter optimization with approximate gradient. In *International Conference on Machine Learning*, pp. 737–746, 2016.
- Rubinstein, B. I., Nelson, B., Huang, L., Joseph, A. D., Lau, S.-h., Rao, S., Taft, N., and Tygar, J. D. ANTIDOTE: Understanding and Defending against Poisoning of Anomaly Detectors. In *Proceedings of the 9th ACM SIGCOMM Conference on Internet Measurement*, pp. 1–14. ACM, 2009.
- Russakovsky, O., Deng, J., Su, H., Krause, J., Satheesh, S., Ma, S., Huang, Z., Karpathy, A., Khosla, A., Bernstein, M., et al. ImageNet Large Scale Visual Recognition Challenge. *International Journal of Computer Vision*, 115(3):211–252, 2015.
- Shafahi, A., Huang, W. R., Najibi, M., Suciu, O., Studer, C., Dumitras, T., and Goldstein, T. Poison Frogs! Targeted Clean-Label Poisoning Attacks on Neural Networks. In *Advances in Neural Information Processing Systems*, pp. 6103–6113, 2018.
- Simard, P. Y., Steinkraus, D., Platt, J. C., et al. Best Practices for Convolutional Neural Networks Applied to Visual Document Analysis. In *ICDAR*, volume 3, 2003.
- Steinhardt, J., Koh, P. W. W., and Liang, P. S. Certified Defenses for Data Poisoning Attacks. In *Advances in Neural Information Processing Systems*, pp. 3517–3529, 2017.
- Xiao, H., Biggio, B., Brown, G., Fumera, G., Eckert, C., and Roli, F. Is Feature Selection Secure against Training Data Poisoning? In *International Conference on Machine Learning*, pp. 1689–1698, 2015.
- Xiao, H., Rasul, K., and Vollgraf, R. Fashion-MNIST: a Novel Image Dataset for Benchmarking Machine Learning Algorithms. *arXiv preprint arXiv:1708.07747*, 2017.
- Xu, H., Caramanis, C., and Mannor, S. Sparse Algorithms Are Not Stable: A No-Free-Lunch Theorem. *IEEE Transactions on Pattern Analysis and Machine Intelligence*, 34(1):187–193, 2011.
- Yao, Y., Viswanath, B., Cryan, J., Zheng, H., and Zhao, B. Y. Automated Crowdturfing Attacks and Defenses in Online Review Systems. In *Proceedings of the 2017 ACM SIGSAC Conference on Computer and Communications Security*, pp. 1143–1158. ACM, 2017.

## A. Hessian-Vector Products

Let  $\mathbf{x} \in \mathbb{R}^m$ ,  $\mathbf{y} \in \mathbb{R}^n$ ,  $\mathbf{v} \in \mathbb{R}^m$ , and  $f(\mathbf{x}, \mathbf{y}) \in \mathbb{R}$ . The Hessian-vector product  $(\nabla_{\mathbf{y}} \nabla_{\mathbf{x}} f(\mathbf{x}, \mathbf{y}))^{\top} \mathbf{v}$  can be efficiently computed by using the following identity (Pearlmutter, 1994):

$$(\nabla_{\mathbf{y}} \nabla_{\mathbf{x}} f(\mathbf{x}, \mathbf{y}))^{\top} \mathbf{v} = \nabla_{\mathbf{y}} (\mathbf{v}^{\top} \nabla_{\mathbf{x}} f(\mathbf{x}, \mathbf{y})). \quad (7)$$

## B. Hypergradient Descent/Ascent Algorithm

Alg. 1 describes the procedure to solve the multiobjective bilevel problem for a particular concentration of poisoning points, via projected hypergradient descent/ascent. In this case,  $\Lambda$  denotes the regularisation hyperparameters. Specifically, `hypGradXp` and `hypGradL` refer to the particular optimisation algorithms used to compute the corresponding hypergradients, and let  $\mathbf{w} \sim p(\mathbf{w}^{(0)})$  be a particular initialisation for the weights. Furthermore, we consider the optimisation of a batch of  $n_p$  poisoning points,  $\mathbf{X}_p = \{\mathbf{x}_p\}_{n=1}^{n_p}$ , simultaneously. This procedure can be repeated for different ratios of poisoning samples.

In our experiments, to sweep different concentrations of poisoning points, we start from the previous poisoned set  $\mathcal{D}'_{tr}$  (for the initial concentration of malicious points,  $\mathcal{D}'_{tr} = \mathcal{D}_{tr}$ ) and substitute  $n_p$  clean samples uniformly sampled without repetition by the initial values of the current  $\mathcal{D}_p$ . We assume that the initial values of the current batch of attack samples  $\mathcal{D}_p$  is given by cloning them from the validation set, and that they are modified according to the space of feasible modifications  $\Phi(\mathbf{X}_p)$ . Their labels are initially flipped and kept fixed during the optimisation. This process is carried out in the function `initXp` in Alg. 1.

In this sense, we simulate different ratios of poisoning points in a cumulative fashion, so that once the optimisation of the previous set of malicious points and  $\lambda$  is finished—event given by the number of hyperiterations to solve the multiobjective bilevel problem—the previous set of malicious points is fixed and the next batch of poisoning points is substituted into the remaining clean training set, to carry out their corresponding optimisation. On the regularisation side, the value of  $\lambda$  continues being updated for the whole set of batches of poisoning points, so as to guarantee the continuity of the optimisation (given that  $\lambda$  needs to be re-adapted to these new perturbed points).

## C. Reverse-Mode and Forward-Mode Differentiation Algorithms

Here we include the Reverse-Mode Differentiation (RMD) algorithm (Alg. 2) that we use to compute the approximate hypergradient at the outer level problem, both for  $\mathbf{X}_p$  and the hyperparameters  $\Lambda$ . The resulting algorithm for the case of  $\Lambda$  is analogous. We also include the Forward-Mode

Algorithm 1. Hypergradient Descent/Ascent

---

**Input:**  $\mathcal{L}, \mathcal{A}, \mathcal{D}_{tr}, \mathcal{D}_{val}, n_p, \Lambda^{(0)}, T$   
**Output:**  $\mathcal{D}_p, \Lambda$   
 $\mathcal{D}'_{tr} \leftarrow \text{initXp}(\mathcal{D}_{val}, n_p)$   
 $\Lambda \leftarrow \Lambda^{(0)}$   
**for** number of hyperiterations **do**  
      $\mathbf{w} \sim p(\mathbf{w}^{(0)})$   
      $\nabla_{\mathbf{X}_p} \mathcal{A} \leftarrow \text{hypGradXp}(\mathcal{L}, \mathcal{A}, \mathcal{D}'_{tr}, \mathcal{D}_{val}, \Lambda, T)$   
      $\mathbf{X}_p \leftarrow \Pi_{\Phi(\mathbf{X}_p)}(\mathbf{X}_p + \alpha \nabla_{\mathbf{X}_p} \mathcal{A})$   $\mathbf{w} \sim p(\mathbf{w}^{(0)})$   
      $\nabla_{\Lambda} \mathcal{A} \leftarrow \text{hypGradL}(\mathcal{L}, \mathcal{A}, \mathcal{D}'_{tr}, \mathcal{D}_{val}, \Lambda, T)$   
      $\Lambda \leftarrow \Pi_{\Phi(\Lambda)}(\Lambda - \beta \nabla_{\Lambda} \mathcal{A})$   
**end for**

---

Algorithm 2. Reverse-Mode Differentiation

---

**Input:**  $\mathcal{L}, \mathcal{A}, \mathcal{D}'_{tr}, \mathcal{D}_{val}, \Lambda, T$   
**Output:**  $\nabla_{\mathbf{X}_p} \mathcal{A}(\mathbf{w}^{(T)})$   
**for**  $t = 0$  **to**  $T - 1$  **do**  
      $\mathbf{w}^{(t+1)} \leftarrow \mathbf{w}^{(t)} - \eta \nabla_{\mathbf{w}} \mathcal{L}(\mathbf{w}^{(t)})$   
**end for**  
 $\mathbf{dX}_p \leftarrow \mathbf{0}$   
 $\mathbf{dw} \leftarrow \nabla_{\mathbf{w}} \mathcal{A}(\mathbf{w}^{(T)})$   
**for**  $t = T - 1$  **down to**  $0$  **do**  
      $\mathbf{A} \leftarrow (\nabla_{\mathbf{w}}^2 \mathcal{L}(\mathbf{w}^{(t)})) \mathbf{dw}$   
      $\mathbf{B} \leftarrow (\nabla_{\mathbf{X}_p} \nabla_{\mathbf{w}} \mathcal{L}(\mathbf{w}^{(t)}))^{\top} \mathbf{dw}$   
      $\mathbf{dX}_p \leftarrow \mathbf{dX}_p - \eta \mathbf{B}$   
      $\mathbf{dw} \leftarrow \mathbf{dw} - \eta \mathbf{A}$   
**end for**  
 $\nabla_{\mathbf{X}_p} \mathcal{A}(\mathbf{w}^{(T)}) \leftarrow \mathbf{dX}_p$

---

Algorithm 3. Forward-Mode Differentiation

---

**Input:**  $\mathcal{L}, \mathcal{A}, \mathcal{D}'_{tr}, \mathcal{D}_{val}, \Lambda, T$   
**Output:**  $\nabla_{\Lambda} \mathcal{A}(\mathbf{w}^{(T)})$   
 $\mathbf{d}\Lambda \leftarrow \mathbf{0}$   
**for**  $t = 0$  **to**  $T - 1$  **do**  
      $\mathbf{A} \leftarrow (\nabla_{\mathbf{w}}^2 \mathcal{L}(\mathbf{w}^{(t)})) \mathbf{d}\Lambda$   
      $\mathbf{B} \leftarrow \nabla_{\Lambda} \nabla_{\mathbf{w}} \mathcal{L}(\mathbf{w}^{(t)})$   
      $\mathbf{d}\Lambda \leftarrow \mathbf{d}\Lambda - \eta (\mathbf{A} + \mathbf{B})$   
      $\mathbf{w}^{(t+1)} \leftarrow \mathbf{w}^{(t)} - \eta \nabla_{\mathbf{w}} \mathcal{L}(\mathbf{w}^{(t)})$   
**end for**  
 $\mathbf{dw} \leftarrow \nabla_{\mathbf{w}} \mathcal{A}(\mathbf{w}^{(T)})$   
 $\nabla_{\Lambda} \mathcal{A}(\mathbf{w}^{(T)}) \leftarrow (\mathbf{d}\Lambda)^{\top} \mathbf{dw}$

---

Differentiation (FMD) algorithm (Alg. 3) that we apply to compute  $\lambda$  in the Subject. E.1 of the Appendix. We make use of the following notation:  $\mathcal{A}(\mathbf{w}^{(T)}) = \mathcal{A}(\mathcal{D}_{val}, \mathbf{w}^{(T)})$ ,  $\mathcal{L}(\mathbf{w}^{(t)}) = \mathcal{L}(\mathcal{D}'_{tr}, \mathbf{w}^{(t)}, \Lambda)$ .

## D. Experimental Settings

### D.1. Synthetic Example

For the synthetic experiment shown in Sect. 4 we sample our training, validation and test points from two bivariate Gaussian distributions,  $\mathcal{N}(\boldsymbol{\mu}_0, \boldsymbol{\Sigma}_0)$  and  $\mathcal{N}(\boldsymbol{\mu}_1, \boldsymbol{\Sigma}_1)$ , with parameters:

$$\boldsymbol{\mu}_0 = \begin{bmatrix} -3.0 \\ 0.0 \end{bmatrix}, \quad \boldsymbol{\Sigma}_0 = \begin{bmatrix} 2.5 & 0.0 \\ 0.0 & 1.5 \end{bmatrix}$$

$$\boldsymbol{\mu}_1 = \begin{bmatrix} 3.0 \\ 0.0 \end{bmatrix}, \quad \boldsymbol{\Sigma}_1 = \begin{bmatrix} 2.5 & 0.0 \\ 0.0 & 1.5 \end{bmatrix}$$

We use 32 (16 per class) points for training and 64 (32 per class) for validation, and one poisoning point that we compute with RMD and add to the training dataset. Moreover, we use a learning rate and a number of hyperiterations for the poisoning points  $\alpha = 0.4$ ,  $T_{\mathcal{D}_p} = 50$ ; the feasible domain  $\Phi(\mathbf{X}_p) \in [-9.5, 9.5]^2$ ; the learning rate and number of iterations for the inner problem  $\eta = 0.2$ ,  $T = 500$ ; and when evaluating the attack,  $\eta_{tr} = 0.2$ , batch size = 32, and number of epochs = 100. When we apply regularisation, we fix  $\lambda = \log(20) \approx 3$ .

### D.2. MNIST, FMNIST and ImageNet

The details of each dataset are included in Table 1. Moreover, both MNIST ‘0’ vs ‘8’ and Fashion-MNIST (FMNIST) T-shirt vs pullover datasets are normalised between  $[0, 1]$ , whereas the ImageNet dog vs fish set is normalised w.r.t. its training mean and standard deviation, as in (Koh & Liang, 2017).

For all the experiments, we make use of Stochastic Gradient Descent to compute the attack points, and to train the model when evaluating the attack. The details of the attack settings are shown in Table 2, whereas the ones for training are in Table 3. There,  $T_{\mathcal{D}_p}$  denotes the number of hyperiterations at the outer problem when  $\lambda$  is fixed,  $T_\lambda$  when the dataset is clean, and  $T_{\text{mult}}$  when  $\mathbf{X}_p$  and  $\lambda$  are computed sequentially;  $\alpha$  and  $\beta$  are the learning rates for the poisoning points and  $\lambda$ , respectively;  $\Phi(\cdot)$  indicates the corresponding feasible domain;  $\eta$  and  $T$  are the learning rate and the number of iterations for the inner problem; and  $\eta_{tr}$  is the learning rate when evaluating the attack.

## E. Additional Results

### E.1. Comparison of Exact Hypergradient, Reverse-Mode and Forward-Mode Differentiation to Update the Regulariser

Given the dimensionality of the poisoning points, we set RMD as the method to optimise them because it is much more efficient in time. For consistency with this method, for

the main experiments of this work we also make use of RMD to compute the value of  $\lambda$  that minimises the multiobjective bilevel problem. However, it is interesting to compare the performance of this method with the other baselines described in Subsect. 3.2, i.e. FMD, and the exact hypergradient (with the conjugate gradient approach), in order to gain intuition about how accurate is the solution obtained by RMD. For the latter, it is also possible to avoid storing the trajectory of the weights—lessening the memory burden—by computing them directly during the backward pass, by reversing the steps followed by the learning algorithm to update them (Muñoz-González et al., 2017). Computing the weights in reverse order w.r.t. the forward step is clearly feasible only if the learning procedure can be exactly traced backwards. We also compare its performance.

We apply Alg. 1 to test this experiment on an LR classifier evaluated on MNIST, where in this case `hypGradL` corresponds to the particular hyperparameter optimisation technique to update  $\lambda$ . To compute the exact hypergradient, we make use of full batch training, with  $T = 1500$  and  $\eta_{tr} = 10^{-2}$ .

In Fig. 4 we represent the performance of RMD, RMD without storing the weights, FMD, and the exact hypergradient. As we can observe, the exact hypergradient approach leads to a lower test error (stronger regulariser), but at the price of requiring a higher number of inner iterations (stronger stationary conditions). This is due to the fact that  $\lambda$  increases faster for the same concentration of malicious points—at the risk of underfitting the clean dataset—as we can see in the right plot. Besides, it is evident that RMD and FMD are equivalent if, during the back-gradient optimisation, we store the trajectory of the weights. On the other hand, in this case not storing the weights leads also to a good approximation of the test error. It is however noteworthy that SGD with fixed step can be shown to be theoretically not reversible (although for linear classifiers and small neural nets it can work in practice, as in (Muñoz-González et al., 2017)). In this work we use SGD with fixed step and store the whole trajectory of the weights, which is primarily critical for deep networks, as reversing the weights trajectory can easily diverge given the strong nonconvexity of the model. There are other strategies such as checkpointing (Maclaurin et al., 2015) that we do not apply here, and we leave as a future research line the study of these strategies in order to reduce the memory requirements of the approach.

### E.2. Test False Positive and False Negative Rate

#### E.2.1. LOGISTIC REGRESSION

In Fig. 5 we represent the results for the test false positive and false negative rate for LR on MNIST, FMNIST, and ImageNet. The results are consistent with the test error shown in Fig. 2, for both rates, the plots for  $\lambda_{\text{RMD}}$  lower bound the

Name	# Training Examples	# Validation Examples	# Test Examples	# Features
MNIST ('0' vs '8')	256/256	256/256	980/974	784
FMNIST ( <i>T-shirt</i> vs <i>pullover</i> )	256/256	256/256	1,000/1,000	784
ImageNet ( <i>dog</i> vs <i>fish</i> )	256/256	256/256	300/300	2,048

Table 1. Characteristics of the datasets used in the experiments.

Name	$T_{\mathcal{D}_p}$	$T_\lambda$	$T_{\text{mult}}$	$\alpha$	$\beta$	$\Phi(\mathbf{X}_p)$	$\Phi(\lambda)$	$\eta$	$T$
MNIST ('0' vs '8') (LR)	100	50	100	0.99	0.99	$[0.0, 1.0]^{784}$	$[-8, \log(200)]$	0.10	150
FMNIST ( <i>T-shirt</i> vs <i>pullover</i> ) (LR)	100	50	100	0.99	0.99	$[0.0, 1.0]^{784}$	$[-8, \log(200)]$	0.10	180
ImageNet ( <i>dog</i> vs <i>fish</i> ) (LR)	100	50	200	0.90	0.40	$[-0.5, 0.5]^{2,048}$	$[-8, \log(20,000)]$	0.05	200
ImageNet ( <i>dog</i> vs <i>fish</i> ) (DNN)	100	75	150	0.99	0.05	$[-0.5, 0.5]^{2,048}$	$[-8, \log(60)]$	0.01	600

Table 2. Experimental settings for the attack.

Name	$\eta_{\text{tr}}$	batch size	number of epochs
MNIST ('0' vs '8') (LR)	$10^{-2}$	64	200
FMNIST ( <i>T-shirt</i> vs <i>pullover</i> ) (LR)	$10^{-2}$	64	200
ImageNet ( <i>dog</i> vs <i>fish</i> ) (LR)	$10^{-3}$	64	300
ImageNet ( <i>dog</i> vs <i>fish</i> ) (DNN)	$10^{-4}$	64	4,000

Table 3. Experimental settings for training the models.

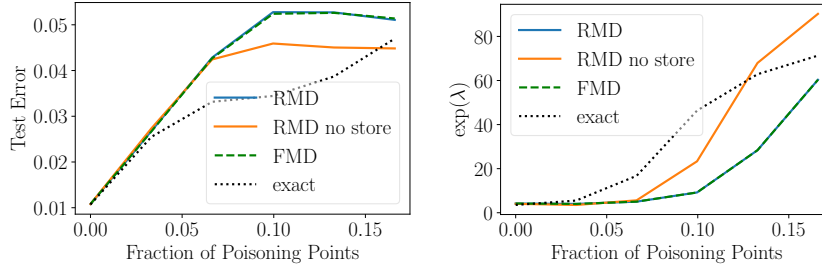


Figure 4. Comparison of optimisation methods to compute the regularisation hyperparameter against the optimal attack on the LR classifier on MNIST, as a function of the concentration of the poisoning points. On the left side we can observe the test error after solving the multiobjective problem, whereas the computed value for  $\lambda$  is on the right side.

corresponding ones when no regularisation is applied. When learning  $\lambda$  for MNIST, after a 10% of poisoning samples the attack appears to focus more on increasing the false positive rate. On the other side, for MNIST, learning  $\lambda$  appears to be more critical on the false positive rate (classifying '0's as '8's), as over-regularising leads to a greater rate up to a roughly 6% of poisoning points; whereas the opposite effect happens for FMNIST and ImageNet: When over-regularising, the false negative rate (classifying pullovers as T-shirts and fishes as dogs, respectively) is greater up to an approximately 5% of poisoning samples.

## E.2.2. DEEP NEURAL NETWORKS

In Fig. 6 we depict the results for the test false positive and false negative rate for the Deep Neural Network (DNN) on ImageNet. The results present a similar trend to the test error (Fig. 3), as again the rates for  $\lambda = -8$  are lower bounded by the ones for  $\lambda_{\text{RMD}}$ . After a roughly 13% of poisoning points, both rates slightly decrease when the fraction of poisoning points increases, as explained in Subsect. 5.2—a significant increase on the regularisation terms can imply an important change in the decision boundary of the DNN. In a similar manner than the case for LR on ImageNet, updating  $\lambda$  becomes more crucial for the false negative rate.

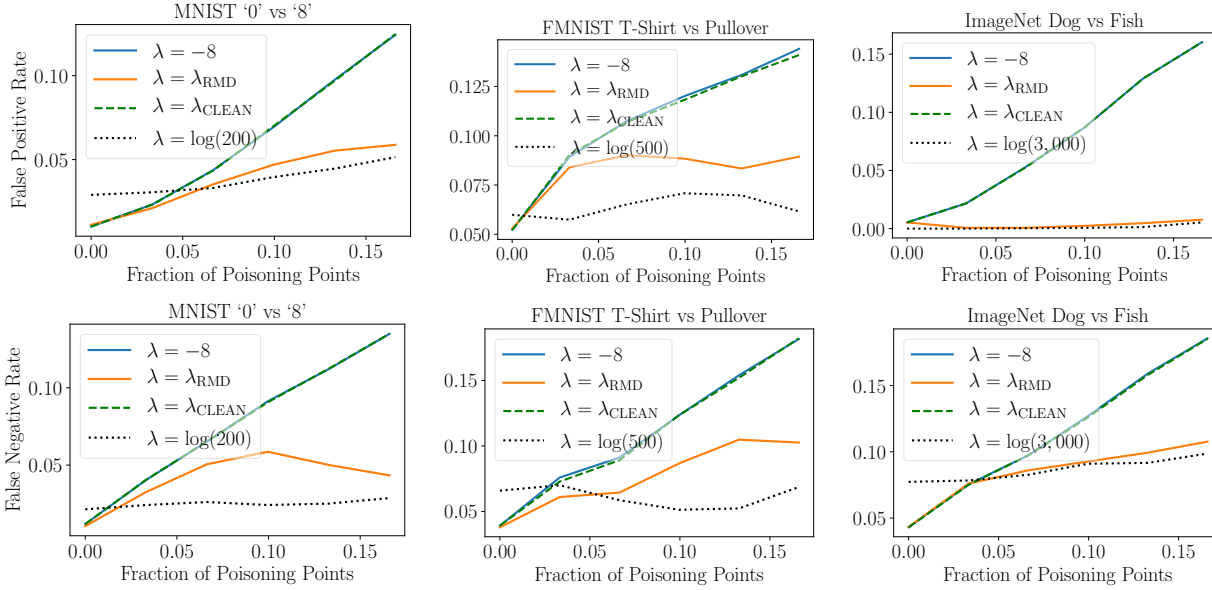


Figure 5. Results for LR on MNIST, FMNIST, and ImageNet.  $\lambda_{\text{RMD}}$  represents the one computed with RMD. The upper row is the test false positive rate, whereas the lower one is the test false negative rate.

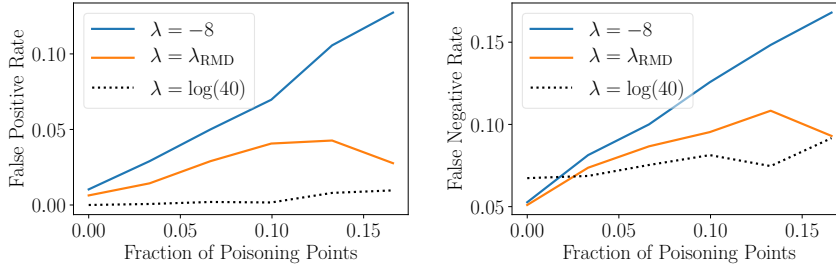


Figure 6. Results for the DNN on ImageNet.  $\lambda_{\text{RMD}}$  represents the one computed with RMD. The left figure is the test false positive rate, whereas the right one is the test false negative rate.

### E.3. Histograms of the Models' Parameters

#### E.3.1. LOGISTIC REGRESSION

In Fig. 7 we represent the histogram of the weights of the LR model, for the clean dataset (blue bars) and when a 16.6% of poisoning points is substituted in the training set (orange bars). To appreciate better the distribution of the parameters, we omitted the upper part of some plots. The first row depicts the cases when no regularisation is applied, and the second row when  $\lambda$  is computed using RMD. We can clearly appreciate the effect of the regularisation: for all the datasets the range of values of  $w$  is narrowed down, and when the attacker poisons the data, this forces the model to even compress more these values down to 0, as the value of  $\lambda$  increases, leading to more stable models.

#### E.3.2. DEEP NEURAL NETWORKS

In Fig. 8 we represent the histogram of the weights of the DNN model on ImageNet dog vs fish, for the clean dataset (blue bars) and when a 16.6% of poisoning points is substituted in the training set (orange bars). The first, second, and third column show the results for the first hidden layer, second hidden layer, and output layer, correspondingly. The first row depicts the cases where no regularisation is applied, and the second row when  $\lambda$  is computed using RMD. Once again, we can appreciate the effect of the regularisation: for all the layers the range of values of  $w$  is narrowed down, and when the attacker poisons the data, this forces the model to even compress more these values.

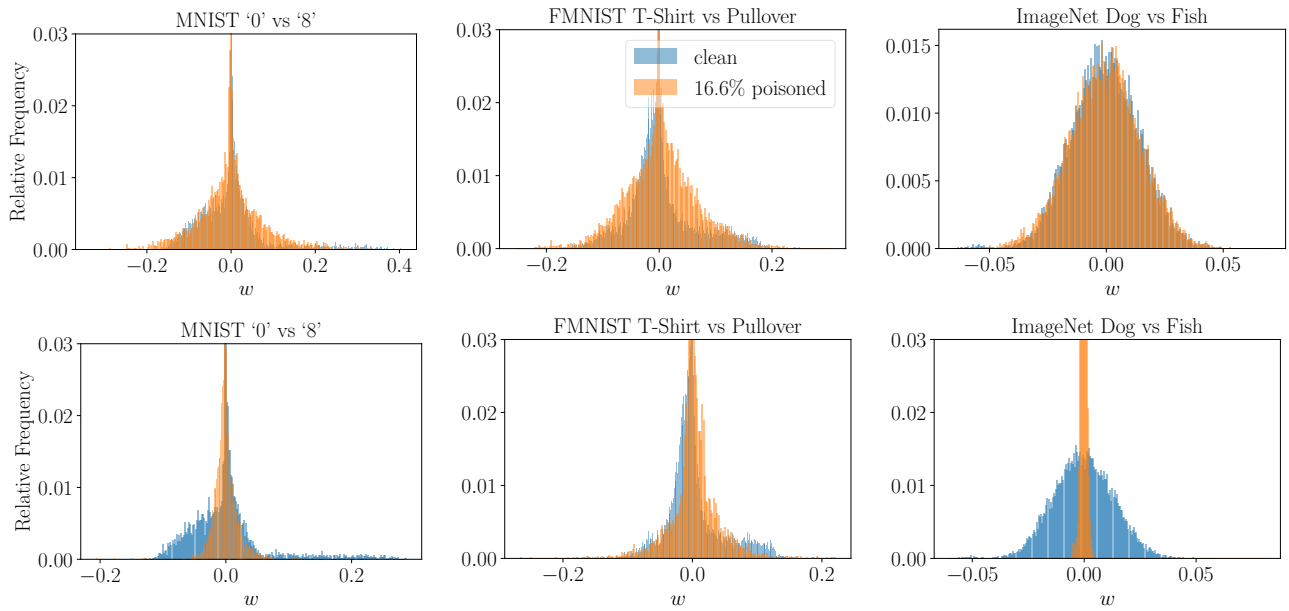


Figure 7. Histograms of the LR’s parameters on MNIST ‘0’ vs ‘8’, FMNIST T-shirt vs pullover, and ImageNet dog vs fish. The first row represents the case where no regularisation is applied, and the second row shows the case where  $\lambda$  is computed with RMD. For a better visualisation, the upper part of some figures has been omitted.

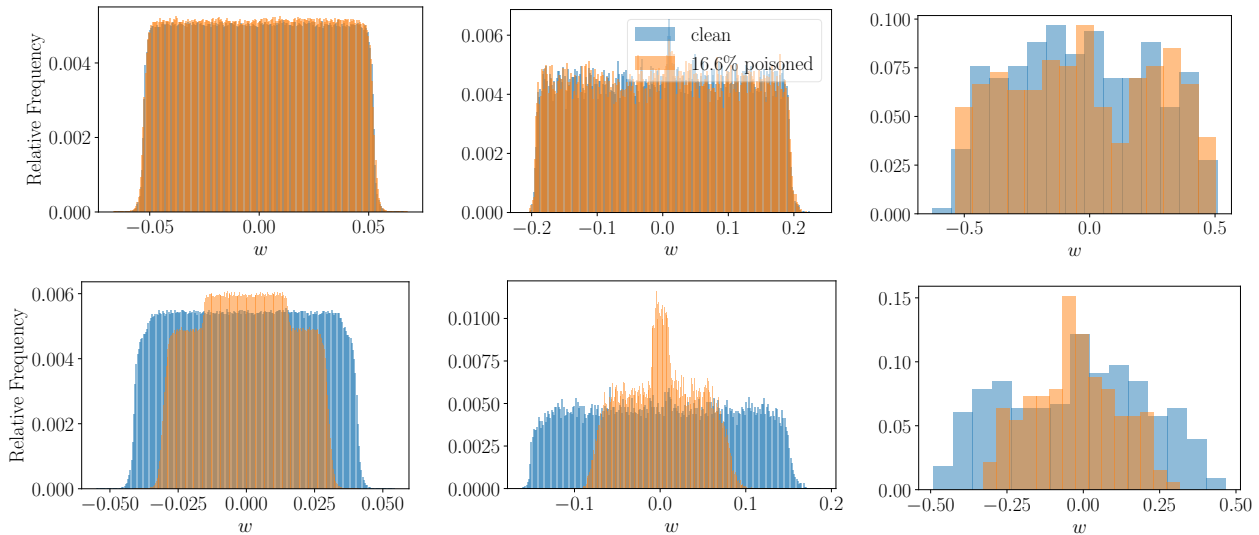


Figure 8. Histograms of the DNN’s parameters on ImageNet. The first, second and third column correspond to the first hidden layer, second hidden layer, and output layer, respectively. The first row represents the case where no regularisation is applied, and the second row shows the when  $\lambda$  is computed with RMD.